2005

Theoretical and numerical perspectives and field observations for the design and performance evaluation of embankments constructed on soft marine clay

Buddhima Indraratna
University of Wollongong, indra@uow.edu.au

Iyathurai Sathananthan
University of Wollongong

C. Bamunawita
University of Wollongong

A. S. Balasubramaniam
Griffith University

Publication Details

This book chapter was originally published as Indraratna, B, Sathananthan, I, Bamunawita, C and Balasubramaniam, AS, Theoretical and numerical perspectives and field observations for the design and performance evaluation of embankments constructed on soft marine clay, in Indraratna and Chu (eds), Ground Improvement - Case Histories, Elsevier, 2005, 199-230. Original book available here.

Chapter 2

Theoretical and Numerical Perspectives and Field Observations for the Design and Performance Evaluation of Embankments Constructed on Soft Marine Clay

B. Indraratna[1], I. Sathananthan[2], C. Bamunawita[2] and A. S. Balasubramaniam[3]

[1]*Professor*, [2]*Former Student*, *School of Civil Engineering, University of Wollongong, NSW 2522, Australia.*
[3]*Professor, School of Engineering, Griffith University, Gold Coast, QLD 4111, Australia.*

ABSTRACT

In this chapter, a two-demensional plane strain solution is adopted for the embankment analysis, which includes the effects of smear zone caused by mandrel driven vertical drains. The equivalent (transformed) permeability coefficients are incorporated in finite element codes, employing modified Cam-clay theory. Selected numerical studies have been carried out to study the effect of embankment slope, construction rate, and drain spacing on the failure of the soft clay foundation. Finally, the observed and predicted performances of well-instrumented full-scale trial embankments built on soft Malaysian marine clay have been discussed in detail. The predicted results agree with the field measurements.

1. INTRODUCTION

The rapid development and associated urbanization have compelled engineers to construct earth structures, including major highways, over soft clay deposits of low bearing capacity coupled with excessive settlement characteristics. In the coastal regions of Australia and Southeast Asia, soft clays are widespread and particularly in the vicinity of capital cities. Because soft soils are weak, unreinforced embankments can only be built 4–5 m high. However, higher embankments are often needed and their rapid construction is pertinent given the usual stringent deadlines. To achieve these goals, special construction measures such as light-weight embankment fill, the provision of reinforcement at the bottom of the embankment, and suitable ground improvement techniques and staged embankment construction must be considered. The application of prefabricated vertical drains (PVDs) with preloading (vacuum pressure or surcharge) has become common practice and is one of the most effective techniques for ground improvement.

Many improvement techniques have been developed to suit particular soil condition, with most soft clay methods based on consolidation. Preloading with vertical drains is a successful ground improvement technique, which involves the loading of the ground surface to induce most of the ultimate settlement of the underlying soft formation. Usually, a surcharge load equal to or greater than the expected foundation loading is applied to accelerate consolidation with the aid of vertical drains. The application of vacuum pressure can reduce the amount of surcharge fill material required to obtain the same consolidation settlement because it generates suction, which increases the effective stress and accelerates consolidation.

Consolidation of soil is the process of decreasing the volume in saturated soils by expelling the pore water. Therefore, the consolidation rate is governed by the compressibility, permeability, and length of the drainage path. The settlement level is directly related to the void ratio change, which is directly proportional to the rate of dissipation of excess pore water pressure. For three decades, vertical drains with preloading have been used to accelerate the consolidation process before commencing construction.

Preloading on its own can reduce the total and differential settlement facilitating the choice of foundations, but when vertical drains are used with preloading, the settlement process can be accelerated considerably (Figure 1). The main advantages of vertical drains are: (i) to increase the shear strength of soil through a decreased void ratio and moisture content; (ii) to decrease the time for preloading to minimize the same level of postconstruction settlement; (iii) to reduce differential settlement during primary consolidation; and (iv) to curtail the height of surcharge fill required to achieve desired precompression.

2. INSTALLATION AND MONITORING OF VERTICAL DRAINS

Before installing vertical drain it is essential that the site be prepared. This may involve removing surface vegetation and debris and grading the site for a sand blanket to act as a medium for expelling water from the drains and an appropriate working mat. The vertical drains can be installed by either the washing jet method, the static method or the dynamic method. The washing jet method is primarily used when installing large diameter sand drains, whereby sand is washed in through the jet pipe. PVDs are usually installed by the static or dynamic method (Figure 2). In the latter, the mandrel is driven into the ground with either a vibrating or drop hammer, but in the former, the mandrel is pushed into the soil by a static load. The static method usually causes less ground disturbances and is preferred for

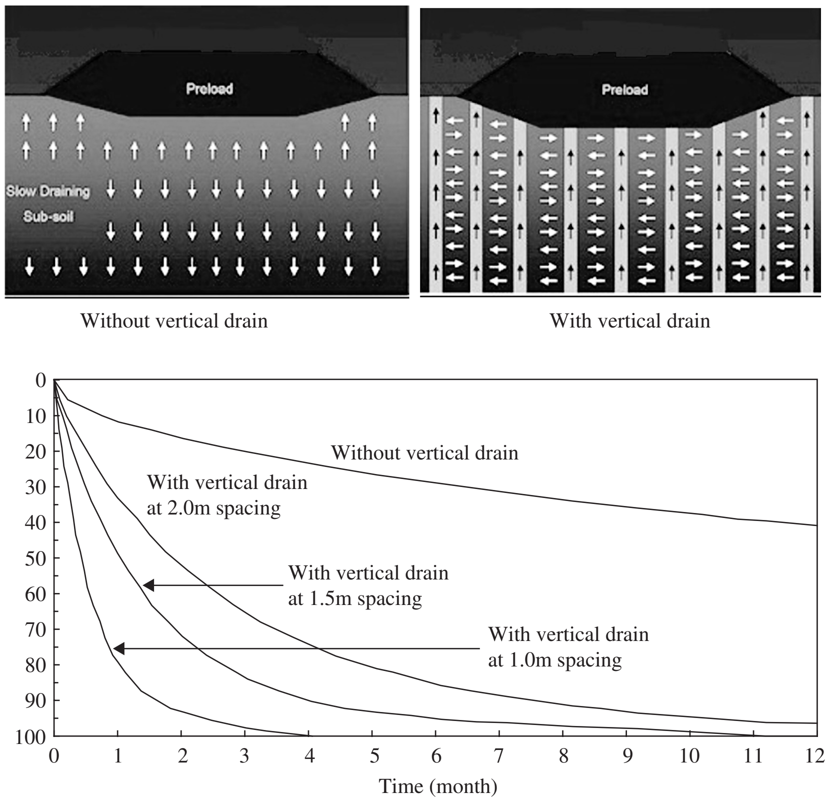

Figure 1. Potential benefit of vertical drains (adapted from Lau et al., 2000).

more sensitive soils. Although faster, the dynamic methods generate higher excess pore pressures and a greater disturbance of the soil around the mandrel during installation.

On major projects, instrumentation is essential for verifying performance and observing design amendments, as warranted, to prevent unacceptable displacement. Figure 3 shows a typical scheme of instruments required to monitor the performance of a soft clay foundation beneath an embankment containing PVD. The most commonly used instruments are inclinometers, settlement indicators, and piezometers, as described in the following section.

2.1. Inclinometers

These instruments are used to monitor the lateral (transverse) movements of natural slopes or embankments. An inclinometer casing has a grooved metal or plastic pipe that is placed into a borehole (Dunnicliff, 1988). The space between the wall of the borehole and the casing is backfilled with a sand or gravel grout. The bottom of the pipe must rest on a firm base to achieve a stable point of fixity. To monitor embankment performance, inclinometers

Figure 2. Typical installation rig (Source: Colbond bv, The Netherlands, http://www.colbond-gepsynthetic. com).

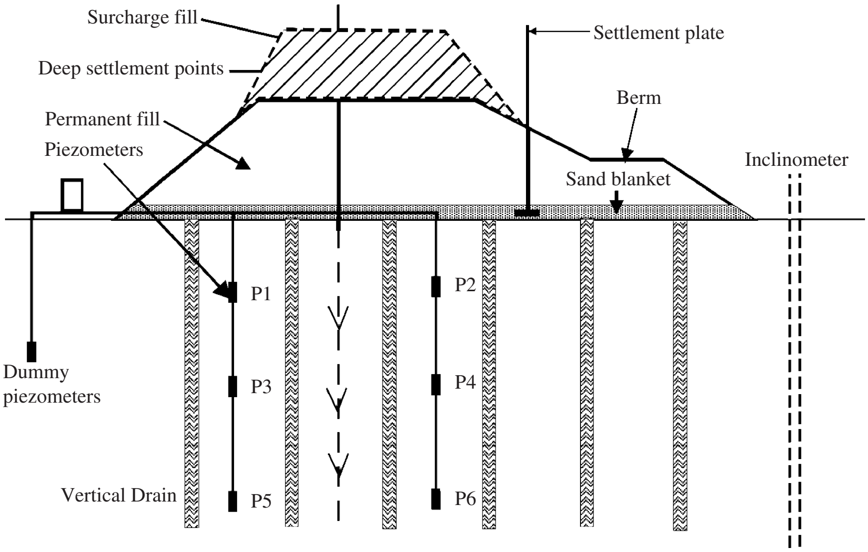

Figure 3. Basic instrumentation for a typical embankment (adapted from Rixner et al., 1986).

are normally placed at or near the toe of the embankment where excessive lateral movement is usually of some concern.

2.2. Settlement indicators

Settlement plates or points are commonly installed where significant settlement is predicted (Dunnicliff, 1988) to record the magnitude and rate of settlement under a load. Therefore, they should be placed immediately after installing the vertical drains. In the simplest form, this instrument is a settlement plate consisting of a steel plate placed on the ground before construction of embankment. Surface settlement points measure vertical displacement with depth, for example, along an embankment centerline. Typically, a reference rod and protecting pipe are attached to the settlement-monitoring platform. Settlement is often evaluated periodically until the surcharge embankment is completed, then at a reduced frequency, measuring the elevation of the top of the reference rod. Benchmarks used for reference datum must be stable and remote from all other possible vertical movements. Further information about settlement points is given elsewhere (Dunnicliff, 1988).

2.3. Piezometers

A detailed description and analysis of various types of piezometers to measure in situ pore water pressure are presented by Hanna (1985) and Dunnicliff (1988). Piezometers should be installed at the bottom of the sand blanket, at various intermediate depths within the compressible layer. A dummy piezometer is usually installed a sufficient distance away from the embankment to record natural groundwater level and excess pore water pressure at a given location is determined by comparison with the "dummy" level.

3. DRAIN PROPERTIES

3.1. Diameter of influence zone

As shown in Figure 4, the equivalent diameter of the influence zone (D_e) can be found in terms of the drain spacing (S) as follows (Hansbo, 1981):

$$D_e = 1.13S \quad \text{for drains installed in a square pattern} \tag{1}$$

and

$$D_e = 1.05S \quad \text{for drains installed in a triangular pattern} \tag{2}$$

Drains in a square pattern may be easier to lay out and control during installation in the field but a triangular pattern usually provides a more uniform consolidation between them.

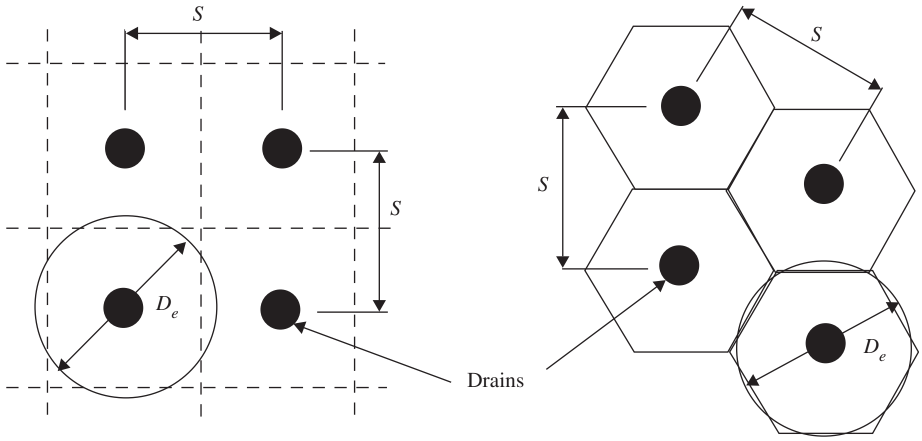

Figure 4. Typical drain installation patterns and the equivalent diameters (adapted from Barron, 1948 and Hansbo, 1981).

3.2. Equivalent drain diameter of band-shaped vertical drain

Most prefabricated drains have rectangular cross-section (band-shaped, Figure 5), but for design purposes, the rectangular (width *a*, thickness *b*) section has to be converted into an equivalent circle with a diameter of d_w, because the conventional theory of radial consolidation assumes that drains are circular.

The following typical equation is used to determine the equivalent drain diameter:

$$d_w = 2(a + b)/\pi \quad \text{(Hansbo, 1979)} \tag{3}$$

Atkinson and Eldred (1981) proposed that a reduction factor of $\pi/4$ should be applied to Eq. (3) to take account of the corner effect, where the flow lines rapidly converge. From the finite element studies, Rixner et al. (1986) proposed that

$$d_w = (a + b)/2 \tag{4}$$

Pradhan et al. (1993) suggested that the equivalent diameter of band-shaped drains should be estimated by considering the flow net around the soil cylinder of diameter d_e (Figure 6). The mean-square distance of their flow net is calculated as

$$s^{-2} = \frac{1}{4}d_e^2 + \frac{1}{12}a^2 - \frac{2a}{\pi^2}d_e \tag{5}$$

$$\text{Then, } d_w = d_e - 2\sqrt{(s^{-2})} + b \tag{6}$$

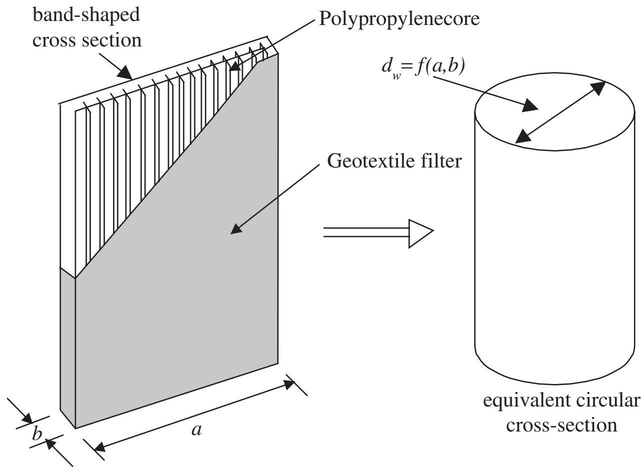

Figure 5. Conceptual drawing of a band-shaped PVD and equivalent diameter well.

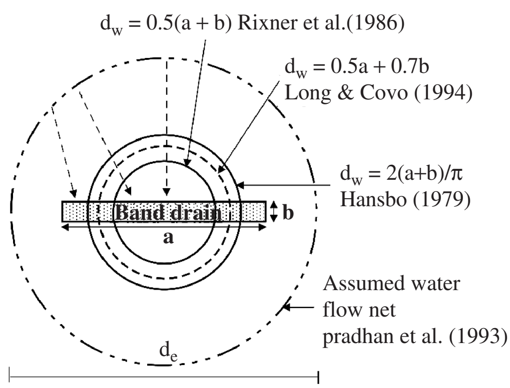

Figure 6. Equivalent diameters of band-shaped vertical drains.

More recently, Long and Covo (1994) found that the equivalent diameter d_w could be computed using an electrical analogue field plotter:

$$d_w = 0.5a + 0.7b \tag{7}$$

3.3. Discharge capacity

The discharge capacity is probably the most important parameter that controls the performance of prefabricated vertical drains. According to Holtz et al. (1991), the discharge capacity depends primarily on the following factors (Figure 7): (i) the area of the drain core available for flow; (ii) the effect of lateral Earth pressure; (iii) possible folding, bending and crimping of the drain; and (iv) infiltration of fine particles into the drain filter.

The current recommended values are given in Table 1 and the discharge capacities of various types of drains are shown in Figure 8 as a function of lateral confining pressure.

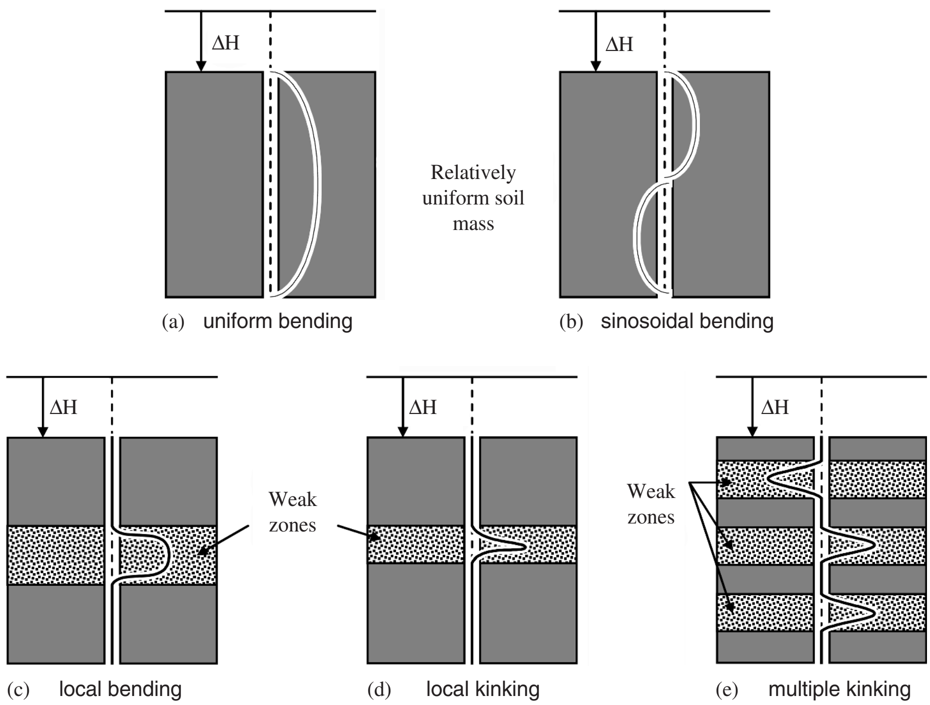

Figure 7. Possible deformation modes of PVD (adapted after Holtz et al., 1991).

Table 1. Current recommended values for specification of discharge capacity

Source	Value	Lateral stress (kPa)
Kremer et al. (1982)	256	100
Kremer (1983)	790	15
Jamiolkowski et al. (1983)	10–15	300–500
Rixner et al. (1986)	100	Not given
Hansbo (1987)	50–100	Not given
Holtz et al. (1989)	100–150	300–500
de Jager and Oostveen (1990)	315–1580	150–300

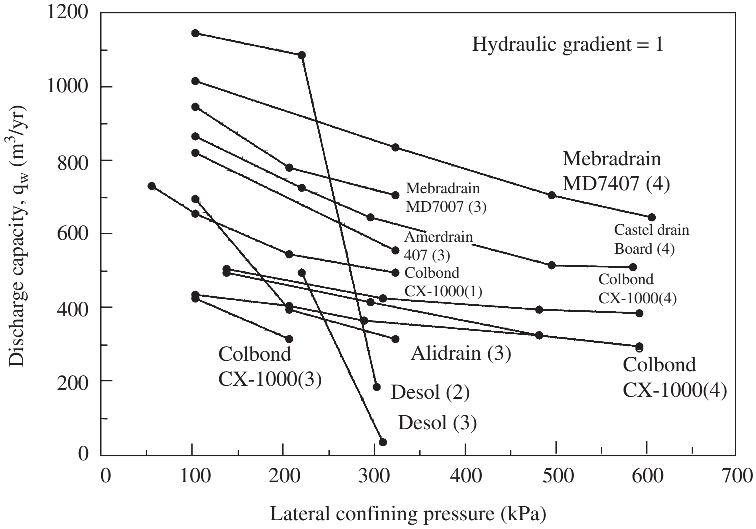

Figure 8. Typical values of vertical discharge capacity (data from Rixner et al., 1986).

4. FACTORS INFLUENCING THE VERTICAL DRAIN EFFICIENCY

4.1. Smear zone

In the field, vertical drains are installed using a steel mandrel, which is pushed into ground statically or dynamically then withdrawn, leaving the drain in the subsoil. This process causes significant remolding of the subsoil, especially in the immediate vicinity of the mandrel. The resulting smear zone will have reduced lateral permeability, which adversely affects consolidation process.

The combined effect of permeability and compressibility within the smear zone causes a different behavior from the undisturbed soil. Predicting soil behavior surrounding the drain requires an accurate estimation of the smear zone properties. In many classical solutions (Barron, 1948; Hansbo, 1981; Indraratna et al., 1997), the influence of the smear zone is considered with an idealized two-zone model.

Two parameters are necessary to characterize the smear effect, namely, the diameter of the smear zone (d_s) and the permeability ratio (k_h/k_s), i.e., the value in the undisturbed zone (k_h) over the smear zone (k_s). Both the diameter of the smear zone and its permeability are difficult to quantify and determine from laboratory tests, and so far, there is no comprehensive or standard method to measure them. The extent of the smear zone and its permeability vary with the installation procedure, size and shape of the mandrel, and the type and sensitivity of soil (macro fabric). Field and laboratory observations (Indraratna and Redana, 1998) indicated a continuous variation of soil permeability with the radial distance away from the drain centreline. Also, the smear zone diameter (d_s) has been the subject of much discussion in literature dealing with PVD.

Investigations by Holtz and Holm (1973) and Akagi (1977) indicate that

$$d_s = 2d_m \tag{8}$$

where d_m is the diameter of the circle with an area equal to the cross-sectional area of the mandrel. Jamiolkowski et al. (1981) proposed that

$$d_s = (2.5 - 3.0)d_m \tag{9}$$

Hansbo (1981, 1997) proposed a different relationship as follows:

$$d_s = (1.5 - 3.0)d_w \tag{10}$$

Based on laboratory study and backanalysis, Bergado et al. (1991) proposed that the following relation could be assumed:

$$d_s = 2d_w \tag{11}$$

Indraratna and Redana (1998) proposed that the estimated smear zone could be as large as $(4–5)d_w$. This proposed relationship was verified using a specially designed large-scale consolidometer (Indraratna and Redana, 1995). Figure 9 shows the variation of k_h/k_v ratio

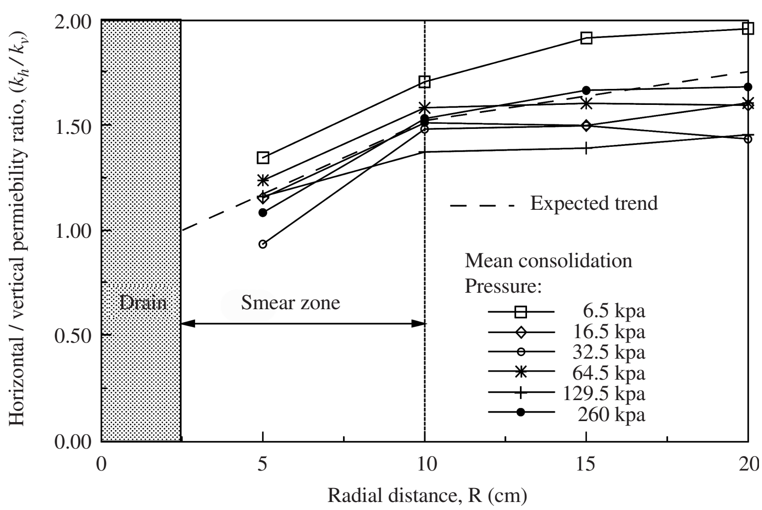

Figure 9. Ratio of k_h/k_v along the radial distance from central drain (modified after Indraratna and Redana, 1998).

along the radial distance from the central drain. According to Hansbo (1987) and Bergado et al. (1991), the k_h/k_v ratio was found to be close to unity in the smear zone. This agrees with the study by Indraratna and Redana (1998). More recently, the primary author and his co-workers at the University of Wollongong attempted to estimate the extent of the smear zone caused by mandrel installation using the Cylindrical Cavity Expansion theory. They used the modified Cam-clay (MCC) model and verified that the extent of smear zone proposed by Indraratna and Redana (1998) was reasonable. Most recent results indicate that for most soft clays the extent of the smear zone is between $4d_w$ and $6d_w$. The recommended smear zone parameters by different researchers are listed in Table 2.

4.2. The effect of a sand mat

Part or all water ingress to drains will flow to the ground first and then drain out through the sand mat. Since the hydraulic conductivity of sand is considerably higher than clay, it can usually be assumed that there is no hydraulic resistance in the sand mat. However, in some cases, depending on local materials, lower quality clayey sand may be used as a sand mat. In these instances, the hydraulic resistance in the sand mat may influence the rate of consolidation of the clay subsoil the amount which is a function of the hydraulic conductivity of the sand as well as the embankment geometry.

4.3. Well resistance

Well resistance refers to the finite permeability of the vertical drain with respect to the soil. Head loss occurs when water flows along the drain and delays radial consolidation. It should be pointed out that well resistance is controlled not only by the discharge capacity of the drain q_w, but also by the permeability of the soil k_h, the maximum discharge length l_m and any geometric deficiencies (bending, kinks, etc.) on the drains.

Table 2. Proposed smear zone parameters

Source	Extent	Permeability	Remarks
Barron (1948)	$r_s = 1.6r_m$	$k_h/k_s = 3$	Assumed
Hansbo (1979)	$r_s = 1.5{\sim}3r_m$	Open	Based on available literature at that time
Hansbo (1981)	$r_s = 1.5r_m$	$k_h/k_s = 3$	Assumed in case study
Bergado et al. (1991)	$r_s = 2r_m$	$k_h/k_v = 1$	Laboratory investigation and backanalysis for soft Bangkok clay
Onoue (1991)	$r_s = 1.6r_m$	$k_h/k_s = 3$	From test interpretation
Almeida et al. (1993)	$r_s = 1.5{\sim}2r_m$	$k_h/k_s = 3{\sim}6$	Based on experience
Indraratna et al. (1998)	$r_s = 4{\sim}5r_m$	$k_h/k_v = 1.15$	Laboratory investigation (for Sydney clay)
Chai and Miura (1999)	$r_s = 2{\sim}3r_m$	$k_h/k_s = C_f(k_h/k_s)$	C_f the ratio between lab and field values
Hird et al. (2000)	$r_s = 1.6r_m$	$k_h/k_s = 3$	Recommend for design
Xiao (2000)	$r_s = 4r_m$	$k_h/k_s = 1.3$	Laboratory investigation (for Kaolin clay)

r_s = radius of smear zone.

Mesri and Lo (1991) proposed the governing equation for vertical flow within the vertical drain in terms of excess pore water pressure at soil–drain interface. Based on Mesri's equation, a well-resistance factor (R) is defined as

$$R = \pi (k_w/k_h)(r_w/l_m)^2 = q_w/(k_h l_m^2) \tag{12}$$

Analysis of the field performance of vertical drains indicated that the well resistance is negligible when $R > 5$. In other words, the minimum discharge capacity $q_{w(min)}$ of vertical drains required for negligible well resistance may be determined from

$$q_{w(min)} = 5 k_h l_m^2 \tag{13}$$

The above relationship is illustrated in Figure 10 for most typical values of k_h and l_m.

Table 3 summarizes the well-resistance indices proposed by various investigators to evaluate the influence of finite discharge capacity of vertical drains. Note that the proposed indices are also transformed to the well-resistance factor (R) proposed by Mesri and Lo (1991). It can be seen that these indices depend on R, except for the expression proposed by Aboshi and Yoshikuni (1967) and Stamatopoulos and Kotzias (1985), in which the drain spacing is also included.

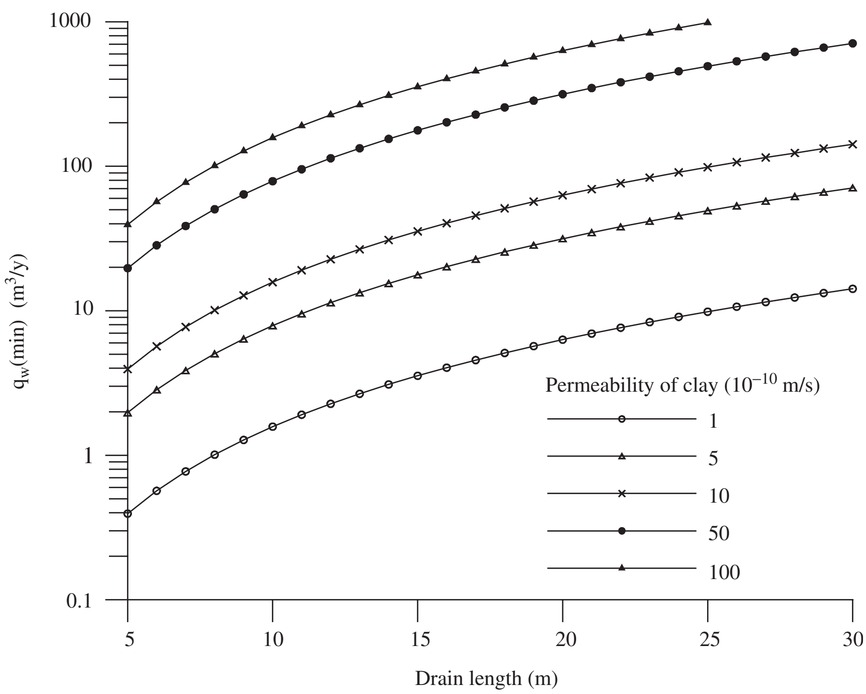

Figure 10. Minimum discharge capacity required (based on Eq. (13)).

Table 3. Summary of proposed well-resistance indices

Source	Index of well resistance
Aboshi and Yoshikuni (1967)	$R_i = \dfrac{(n^2-1)}{4F(n)n^2}\dfrac{k_\mathrm{h}}{k_\mathrm{w}}\left(\dfrac{l_\mathrm{m}}{r_\mathrm{w}}\right)^2 = \dfrac{\pi(n^2-1)}{4F(n)n^2}\dfrac{1}{R}$
Yoshikuni and Nakanodo (1974), Onoue (1988)	$L = \dfrac{8}{\pi^2}\dfrac{k_\mathrm{h}}{k_\mathrm{w}}\left(\dfrac{l_\mathrm{m}}{r_\mathrm{w}}\right)^2 = \dfrac{8}{\pi}\dfrac{1}{R}$
Hansbo (1981)	$W = 2\dfrac{k_\mathrm{h}}{k_\mathrm{w}}\left(\dfrac{l_\mathrm{m}}{r_\mathrm{w}}\right)^2 = 2\pi\dfrac{1}{R}$
Stamatopoulos and Kotzias (1985)	$R_i = \dfrac{1}{F(n)}\dfrac{k_\mathrm{h}}{k_\mathrm{w}}\left(\dfrac{l_\mathrm{m}}{r_\mathrm{w}}\right)^2 = \dfrac{\pi}{F(n)}\dfrac{1}{R}$
Zeng and Xie, (1989)	$\mathrm{G} = \dfrac{1}{4}\dfrac{k_\mathrm{h}}{k_\mathrm{w}}\left(\dfrac{l_\mathrm{m}}{r_\mathrm{w}}\right)^2 = \dfrac{\pi}{4}\dfrac{1}{R}$
Mesri and Lo (1991)	$R = \pi\dfrac{k_\mathrm{w}}{k_\mathrm{h}}\left(\dfrac{r_\mathrm{w}}{l_\mathrm{m}}\right)^2 = \dfrac{q_\mathrm{w}}{k_\mathrm{h} l_\mathrm{m}^2}$

$n = D_\mathrm{e}/d_\mathrm{w}$ is the spacing ratio.

In general, laboratory and field data indicate that the discharge capacities of most commercial PVDs have little influence on the consolidation rate of clay, especially for drains that are not too long (Indraratna et al., 1994). For values of $q_\mathrm{w} > 100$–150 m^3/year (in the field) and where drains are shorter than 30 m, there should be no significant increase in the consolidation time. Given these circumstances, it may be claimed that for commercial PVDs, well resistance is usually negligible in most practical situations unless the drains are excessively long and geometric deficiencies occur during installation (bending, kinks, etc). In most soft clays, well resistance can be ignored for PVD < 15 m long.

5. DEVELOPMENT OF VERTICAL DRAIN THEORY

Analytical solutions already developed for consolidation of ground improved with vertical drains invariably employ the "unit cell" model, as illustrated in Figure 11. The theory for radial drainage consolidation has been addressed by many researchers (Rendulic, 1936; Carrillo, 1942; Barron, 1948; Yoshikuni and Nakanode, 1974; Hansbo, 1981; Onoue, 1988; Zeng and Xie, 1989).

5.1. Rendulic and Carillo diffusion theory

Rendulic (1936) formulated and solved the differential equation for one-dimensional vertical compression by radial flows

$$\frac{\partial u}{\partial t} = c_\mathrm{h}\left(\frac{\partial^2 u}{\partial r^2} + \frac{1}{r}\frac{\partial u}{\partial r}\right) \tag{14}$$

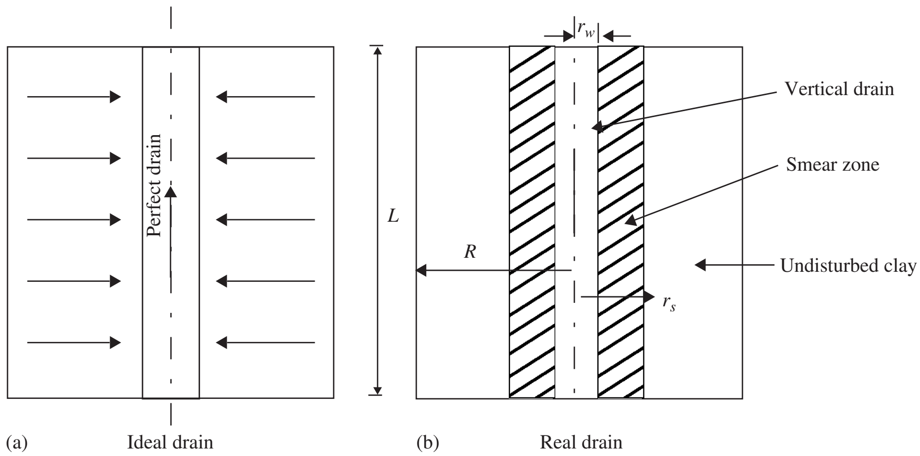

Figure 11. Unit-cell model of a drain surrounding by soil cylinder (after Barron, 1948).

where r is the coordinate and c_h the horizontal coefficient of consolidation ($k_h/\gamma_w m_v$).

Carillo (1942) showed that for radial drainage and associated 1-D consolidation, the excess pore water pressure $u_{r,z}$ is given by

$$\frac{\partial u}{\partial t} = c_h\left(\frac{\partial^2 u}{\partial r^2} + \frac{1}{r}\frac{\partial u}{\partial r}\right) + c_v\frac{\partial^2 u}{\partial z^2} \tag{15}$$

$$u_{r,z} = u_r u_z / u_0 \tag{16}$$

where, u_r and u_z are the excess pore water pressure due to radial flow and vertical flow only, and u_0 is the initial pore water pressure. By substituting the average excess pore water pressure into Eq. (16), the average degree of consolidation of the compressible stratum can be obtained by combining U_z and U_r, hence

$$(1 - \overline{U}) = (1 - \overline{U}_z)(1 - \overline{U}_r) \tag{17}$$

where $\overline{U}$ is the average degree of consolidation of the clay at time t for combined vertical and radial flow, and $\overline{U}_z$ and $\overline{U}_r$ are the average degree of consolidation at time t for vertical and radial flow, respectively. It should be noted that both Rendulic and Carillo's solutions are for "ideal" drains only (infinite discharge capacity with no smear zone).

5.2. Barron's (1948) 'equal strain' rigorous solution

Barron (1948) addressed the smear and well-resistance effects that can decrease the performance of vertical drains. He presented closed-form solutions for two extreme cases for radial drainage-induced consolidation, namely, "free strain" and "equal strain", and showed that the average consolidation obtained in both cases is almost the same.

The "free strain" hypothesis assumes that the load is uniform over a circular zone of influence for each vertical drain. The differential settlements occurring over this zone do not affect the redistribution of stresses caused by the fill load arching. In contrast, the "equal strain" assumes that arching occurs in the upper layer during consolidation without any differential settlement in the clay layer, which is what its simplicity is commonly used by researchers.

Figure 12 shows the schematic illustration of a soil cylinder with a central vertical drain, where r_w is the radius of the drain, r_s is the radius of smear zone, R is the radius of soil cylinder and l is the length of the drain installed into soft ground. The coefficient of permeability in the vertical and horizontal directions are k_v and k_h, respectively, and k'_h is the coefficient permeability in the smear zone. Based on "equal strain", Barron (1948) proposed a solution to Eq. (14) taking the smear effect into account as

$$u_r = \bar{u}\frac{1}{v}\left[\ln\left(\frac{r}{r_s}\right) - \frac{(r^2 - r_s^2)}{2R^2} + \frac{k_h}{k'_h}\left(\frac{n^2 - s^2}{n^2}\right)\ln(s)\right] \tag{18}$$

where the smear factor v is given by

$$v = F(n, s, k_h, k'_h) = \left[\frac{n^2}{n^2 - s^2}\ln\left(\frac{n}{s}\right) - \frac{3}{4} + \frac{s^2}{4n^2} + \frac{k_h}{k'_h}\left(\frac{n^2 - s^2}{n^2}\right)\ln(s)\right] \tag{19}$$

and $$\bar{u} = u_0 \exp\left(-8T_h/v\right) \tag{20}$$

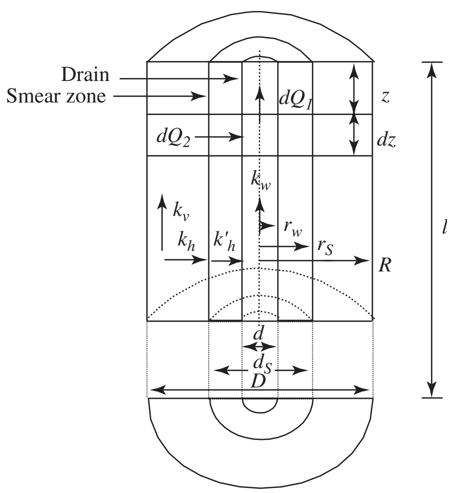

Figure 12. Schematic of soil cylinder with vertical drain (adapted from Hansbo, 1997).

In the above expression, $s = r_s/r_w$, $n=R/r_w$, T_h is the time factor given by $T_h = c_h\, t/4R^2$, $\bar{u}$ the average excess pore water pressure, and u_0 the initial excess pore water pressure.

The average degree of consolidation, $\bar{U}_r$, in the soil body is given by

$$\bar{U}_r = 1 - \exp\left(-\frac{8T_h}{\nu}\right) \tag{21}$$

5.3. *Hansbo (1981) – Analysis with smear and well resistance*

Hansbo (1981) presented an approximate solution for vertical drain based on the "equal strain" by taking both smear and well resistance into consideration. The $\bar{U}_r$, presented by Hansbo (1981), can be expressed as

$$\bar{U}_r = 1 - \exp(-8T_h/\mu) \tag{22}$$

where upon ignoring the insignificance terms, gives

$$\mu = \ln\left(\frac{n}{s}\right) + \left(\frac{k_h}{k'_h}\right)\ln(s) - 0.75 + \pi z(2l - z)\frac{k_h}{q_w} \tag{23}$$

6. 2-D MODELLING OF VERTICAL DRAINS

Even though each vertical drain is axisymmetric, finite element analyses dealing with multidrain embankments have commonly been conducted under "plane strain" conditions for optimizing computational efficiency. Therefore, to employ a realistic 2-D plane strain analysis for vertical drains, the appropriate equivalence between the plane strain and axisymmetric analysis needs to be established in terms of consolidation settlement. Figure 13 shows the conversion of an axisymmetric vertical drain into an equivalent drain wall. This can be achieved in several ways (Hird et al., 1992; Indraratna and Redana, 1997), for example: (i) geometric matching – the drain spacing is matched while maintaining the same permeability coefficient; (ii) permeability matching – coefficient of permeability is matched while keeping the same drain spacing; and (iii) combination of (i) and (ii), with the plane strain permeability calculated for a convenient drain spacing.

6.1. *Shinsha et al. (1982) – permeability transformation*

Shinsha et al. (1982) first proposed an acceptable matching criterion for converting the permeability coefficients. The equivalent coefficient of permeability was calculated on the assumption that the required time for a 50% degree of consolidation in both schemes was the same, giving

$$k_{pl}/k_{ax} = (B/D_e)^2 T_{h50}/T_{r50} \tag{24}$$

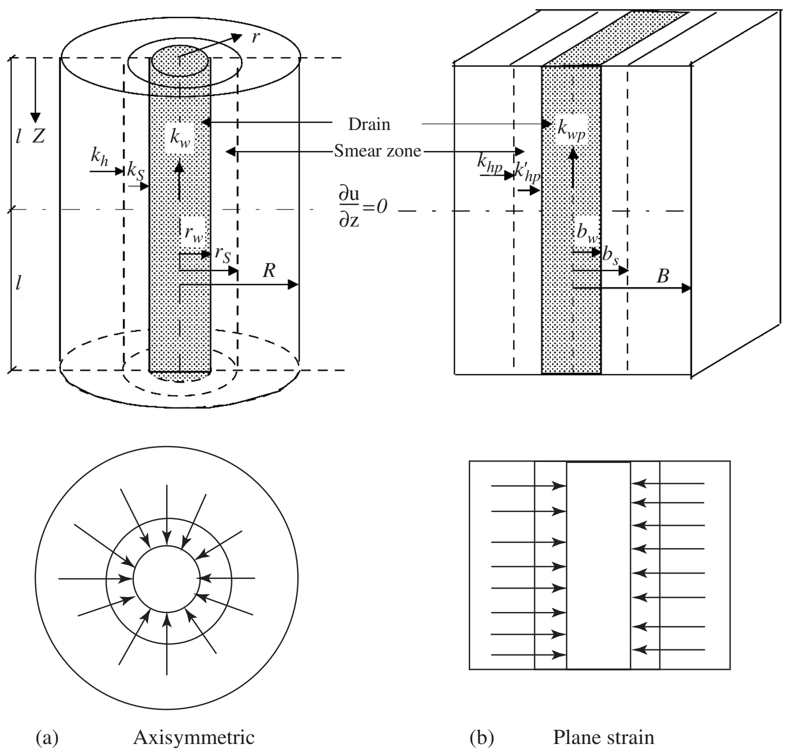

Figure 13. Conversion of an axisymmetric unit cell into plane strain condition (adapted from Hird et al., 1992 and Indraratna and Redana, 1997).

where T_{h50}=0.197 is a dimensionless time factor at 50% consolidation of laminar flow and T_{r50} the corresponding radial flow.

6.2. Hird et al. (1992) – geometry and permeability matching

By adapting Hansbo's (1981) theory for the plane strain case, Hird et al. (1992) showed that the average degrees of consolidation U, at any depth and time in the two unit cells were theoretically identical if well resistance was ignored:

$$\frac{k_{pl}}{k_{ax}} = \frac{2B^2}{3R^2\left[\ln\left(\frac{R}{r_s}\right) + \left(\frac{k_{ax}}{k_s}\right)\ln\left(\frac{r_s}{r_w}\right) - \frac{3}{4}\right]} \tag{25}$$

where subscripts "ax" and "pl" represent the axisymmetric and plane strain conditions, respectively. Note that the geometric matching is achieved by substituting $k_{pl}=k_{ax}=k_h$ in

Eq. (25), whereas the permeability matching is obtained by substituting $B=R$. For incorporating well resistance, the following dimensionless expression can be used:

$$Q_w/q_w = 2B/\pi R^2 \tag{26}$$

6.3. Bergado and Long (1994) – equal discharge concept

The converted permeability, including smear effect, is introduced based on the condition of the equal discharge rate in both schemes and on the assumption that the coefficient of permeability is independent of the seepage state:

$$\frac{k_{pl}}{k_{ax}} = \frac{\pi D(1 - a_s)}{2S\left[\ln\left(\frac{\alpha D}{d_s}\right) + \left(\frac{k_{ax}}{k_s}\right)\ln\left(\frac{d_s}{d_w}\right)\right]} \tag{27}$$

where $a_s=t/D$, t is the thickness of the walls in 2-D model, D and S are the row spacing and pile spacing of the actual case, respectively, $\alpha = D_e/D$, $S = D$ and $\alpha = 1.05$ for square pattern, $S = 0.866D$ and $\alpha = 1.13$ for triangular pattern.

6.4. Chai et al. (1995) – well resistance and clogging

Chai et al. (1995) successfully extended the analysis by Hird et al. (1992) to include the effect of well resistance and clogging. In this approach, the discharge capacity of the drain in plane strain (q_{wp}) for matching the average degree of horizontal consolidation is given by

$$q_{wp} = \frac{4k_h l^2}{3B\left[\ln\left(\frac{n}{s}\right) + \frac{k_h}{k_s}\ln(s) - \frac{17}{12} + \frac{2l^2\pi k_h}{3q_{wa}}\right]} \tag{28}$$

6.5. Kim and Lee (1997) – Time factor analysis

They assume that the time durations for the two systems (plane strain and axisymmetric) to achieve a 50% and 90% degree of consolidation are the same. Then, the following simple expression is obtained:

$$\frac{k_{pl}}{k_{ax}} = \left(\frac{B}{R}\right)^3 \frac{T_{r50}}{T_{h50}} \frac{T_{r90}}{T_{h90}} \frac{S}{\pi d_w} \tag{29}$$

6.6. Indraratna and Redana (1997) – Rigorous solution for parallel drain wall

Indraratna and Redana (1997) converted the vertical drain system shown in Figure 13 into an equivalent parallel drain wall by adjusting the coefficient of soil permeability. They assumed that the half-widths of unit cell B, of drains b_w, and of smear zone b_s are the same as their axisymmetric radii R, r_w and r_s, respectively. The equivalent permeability of the model is then determined by

$$k_{hp} = \frac{k_h\left[\alpha + (\beta)\dfrac{k_{hp}}{k'_{hp}} + (\theta)(2lz - z^2)\right]}{\left[\ln\left(\dfrac{n}{s}\right) + \left(\dfrac{k_h}{k'_h}\right)\ln(s) - 0.75 + \pi(2lz - z^2)\dfrac{k_h}{q_w}\right]} \tag{30}$$

The associated geometric parameters α, β and the flow term θ are given by

$$\alpha = \frac{2}{3}\frac{(n-s)^3}{(n-1)n^2} \tag{31a}$$

$$\beta = \frac{2}{3}\frac{(s-1)}{(n-1)n^2}[3n(n-s-1) + (s^2+s+1)] \tag{31b}$$

and

$$\theta = \frac{2k_{hp}}{Bq_z}\left(1 - \frac{1}{n}\right) \tag{31c}$$

where $q_z = 2q_w/\pi B$ is the equivalent plane strain discharge capacity.

In Eq. (30), as k_{hp} appears on both sides of the equation the solution is obtained by iteration with an initially assumed k_{hp}/k'_{hp} ratio.

To verify the above model a finite element analysis was undertaken for both axisymmetric and equivalent plane strain models. As an example, a unit drain was analyzed with a drain installed to a depth of 5 m below the ground surface at 1.2 m spacing. The model parameters and soil properties were $r_w = 0.03$ m, $r_m = 0.05$ m, $k_h = 1 \times 10^{-8}$ m/s, $k'_h = 5 \times 10^{-9}$ m/s, and the corresponding equivalent coefficients of plane strain permeability were $k'_{hp} = 5.02 \times 10^{-10}$ m/s, and $k_{hp} = 2.97 \times 10^{-9}$ m/s based on Eq. (30). The water table was assumed to be at the surface and $r_s = 5r_m$ (based on experimental results). For the elasto-plastic finite element analysis, MCC model was used as follows: $\lambda = 0.2$, $\kappa = 0.04$, $M = 1.0$, $e_{cs} = 2$ and Poisson's ratio $\nu = 0.25$, with a saturated unit weight of 18 kN/m^3.

The results of both axisymmetric and plane strain analysis are plotted in Figure 14. The average degree of radial consolidation U_h (%) is plotted against the time factor T_h for perfect drain conditions. As illustrated, the proposed plane strain analysis agree perfectly with the axisymmetric analysis, with the maximum deviation between the two methods being less than 5%.

Figures 15 and 16 illustrate the settlements and excess pore pressure variations over time, including smear plus well resistance for a single drain and again the axisymmetric model and the equivalent plane strain model agreed.

Based on the above single drain analysis, Figures 14–16 provide concrete evidence that the equivalent (converted) plane strain model is an excellent substitute for the axisymmetric

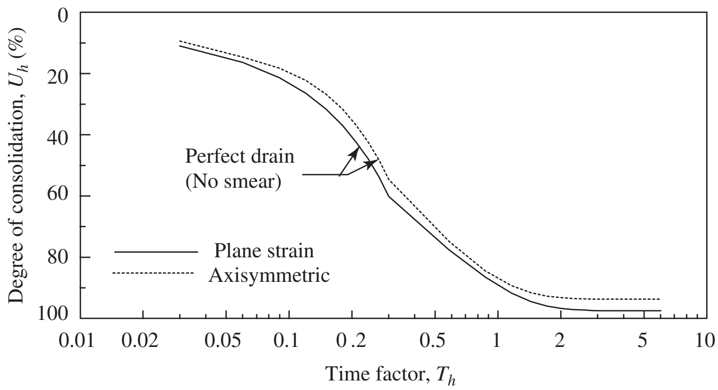

Figure 14. Average degree of consolidation versus time factor (modified after Indraratna et al., 2000).

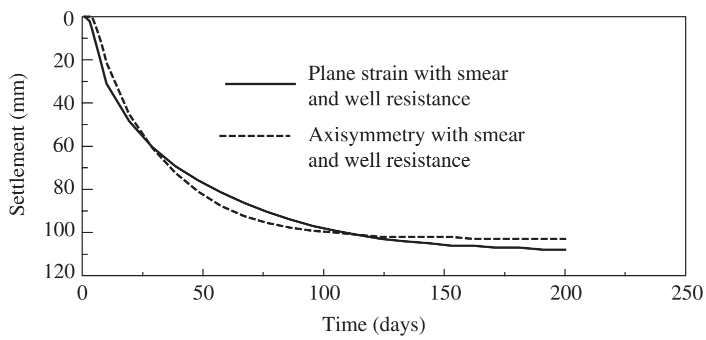

Figure 15. Comparison of the surface settlement (modified after Indraratna et al., 2000).

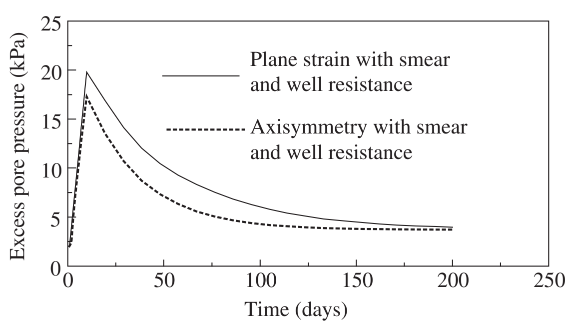

Figure 16. Comparison of the excess pore pressure (modified after Indraratna et al., 2000).

model. In finite element modelling, the 2-D plane strain analysis is expected to reduce computational time considerably compared to the time taken by a 3-D, axisymmetric model, especially in multidrain analysis.

7. SIMPLE 1-D MODELLING OF VERTICAL DRAINS

A simple approximate method for modelling the effect of PVD is proposed by Chai et al. (2001). Because PVD increases the mass permeability of subsoil in the vertical direction, it is logical to establish a value for vertical permeability which approximately represents the effect of vertical drainage of natural subsoil and radial permeability toward the PVD. This equivalent vertical permeability (k_{ve}) was derived from an equal average degree of consolidation under the 1-D condition. To obtain a simple expression for $k_{ve,}$ an approximation equation for consolidation in the vertical direction was proposed:

$$U_v = 1 - \exp(-C_d T_v) \tag{32}$$

where T_v is the time factor for vertical consolidation, and C_d = constant = 3.54. The equivalent vertical permeability, k_{ve}, can be expressed as:

$$k_{ve} = \left(1 + \frac{2.5 l^2 k_h}{\mu D_e^2 k_v}\right) k_v \tag{33}$$

where l is drain length, D_e the equivalent diameter of unit cell, and

$$\mu = \ln\left(\frac{n}{s}\right) + \frac{k_h}{k_s}\ln(s) - \frac{3}{4} + \frac{\pi 2 l^2 k_h}{3 q_w} \tag{34}$$

8. A FINITE ELEMENT MODEL PERSPECTIVE FOR GENERAL DESIGN

Finite element analysis is an important tool for current design processes (Potts and Zdravkovic, 2000). In this section, selected numerical studies have been carried out to study how the embankment slope, construction rate, and drain spacing affect the failure of a soft clay foundation using the finite element code ABAQUS. The subsoil profiles are given in Tables 4 and 5 and the plane strain permeability coefficients are calculated using Eq. (30).

8.1. Element types for soil and soil–drain interface

The types of elements used in consolidation analysis in the finite element code ABAQUS are shown in Figure 17. The basic element type is a four-node bilinear displacement and pore pressure element (CPE4P) consisting of four displacement and pore pressure nodes at

Table 4. Soil properties used in finite element analysis

Depth (m)	Soil type	k_h (10^{-9} m/s)	e_o	λ	κ	ν	M	γ(kN/m^3)
0–2.0	Weathered clay	30.1	1.8	0.3	0.03	0.3	1.2	16.0
2.0–8.5	Very soft clay	12.7	2.8	0.73	0.08	0.3	1.0	14.5
8.5–10.5	Soft clay	6.02	2.4	0.5	0.05	0.25	1.2	15.0
10.5–13.0	Medium clay	2.55	1.8	0.3	0.03	0.25	1.4	16.0
13.0–18.0	Stiff clay	0.60	1.2	0.1	0.01	0.25	1.4	18.0

Table 5. In situ stress condition used in finite element analysis

Depth (m)	σ'_{ho}(kPa)	σ'_{vo}(kPa)	u (kPa)
0	5	5	−5
0.5	8	8	0
2	11	11	15
8.5	28	39.75	80
10.5	35	49.75	100
13.0	49	64.75	125
15.0	57	80.75	145

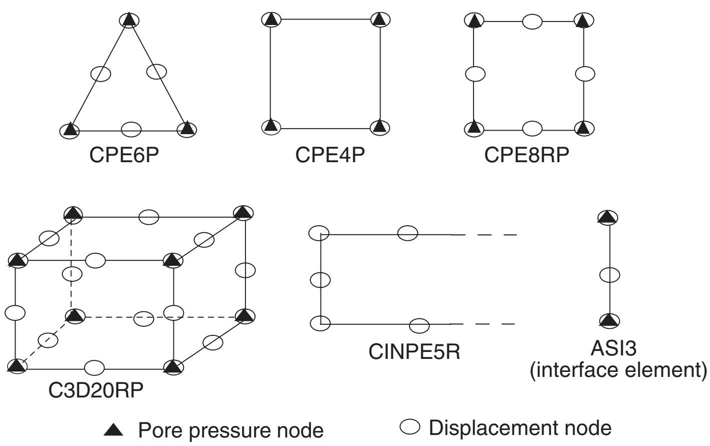

Figure 17. Types of elements used in consolidation analysis (Hibbitt, K. & Sorensen 2004).

the corners. The higher order of this element is a 20-node tri-quadratic displacement and tri-linear pore pressure nodes with reduced integration (C3D20RP), which contain 20 displacement nodes and eight pore pressure nodes. As explained by Hibbitt, K. & Sorensen (2004) reduced integration elements use a lower order of integration to form element stiffness. ABAQUS recommends using reduced integration elements because it usually gives more accurate results and is less time consuming than full integration. The common element type used in the analysis presented here is the CPE8RP element, which contains eight displacement nodes and four pore pressure nodes.

Interface elements are most appropriate to simulate soil–drain interaction. Since the thickness of PVD is relatively small compared to its spacing, the interface element is envisaged as the soil element having properties similar to the adjacent soil except for permeability. A three-node interface element (ASI3) is shown in Figure 17, where there are two pore pressure nodes at the ends.

In finite element analysis, the pore pressure shape function is usually one order less than the displacement shape function. In most of the elements shown in Figure 17, the pore pressure shape function is linear, while the displacement shape functions are either quadratic or cubic.

Figure 18 presents a typical discretized finite element mesh, which is used for numerical analysis, where only one-half of the embankment is considered by symmetry. A foundation depth of 15 m was considered sufficient for analysis, assuming the existence of a stiff clay layer beneath this depth. The mesh consists of more than 1000 CPE8RP elements and the vertical drains are modelled by an interface element (ASI3). A finer mesh was employed for the zone beneath the embankment, with a half-width of 20 m. The embankment loading is simulated by applying incremental vertical loads.

8.2. Embankment constructed on soft clay without any improvement

8.2.1. Effect of the slope of the embankment. To illustrate the effect of embankment slope on foundation failure, two plane strain finite element analyses were conducted using the finite element mesh shown in Figure 18. Two slopes are considered here, 2:1 and 3:1 (horizontal:vertical), and the loading is simulated by a constant rate of 0.1 m/week. Failure is identified when the solution fails to converge and displacement continues to increase without any further load added.

Figure 19 shows the predicted heave at the toe of the embankment based on the two models. A measurable change in settlement rate close to failure is observed and, finally, settlement increases without having to increase the embankment height. The decrease in

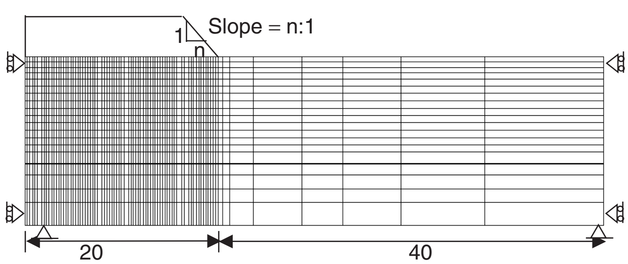

Figure 18. Finite element mesh.

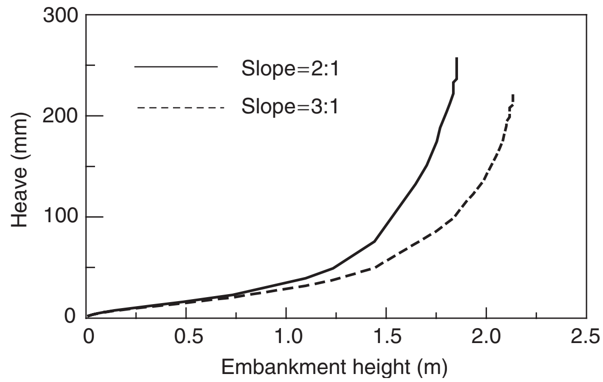

Figure 19. Heave at the toe of the embankment.

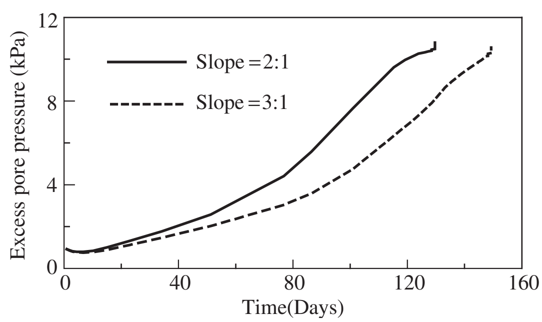

Figure 20. Excess pore pressure distribution 2 m below the embankment toe.

embankment slope has the effect of increasing the embankment height at failure from 1.8 to 2.1 m. Figure 20 presents excess pore pressure distribution at 2 m below ground level at the embankment toe. As expected, excess pore pressure increment is not gradual and a sudden increase is observed because the point considered here is located within the expected failure zone. Predicted surface settlement profile at failure based on these two models is presented in Figure 21.

8.2.2. ***Effect of loading rate of the embankment.*** To study the effect of construction rate of the embankment on failure height, plane strain finite element analysis was conducted for the two different construction rates, 0.1 m/week and 0.35 m/week, for an embankment slope of 3:1. The predicted heave at the toe of the embankment is shown in Figure 22. The slow rate of construction permits a greater embankment height at failure,

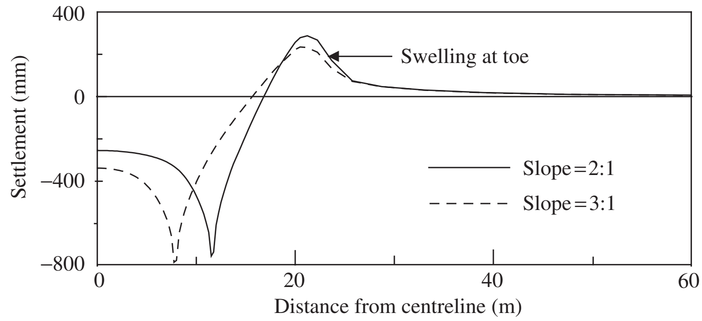

Figure 21. Surface settlement profile at failure.

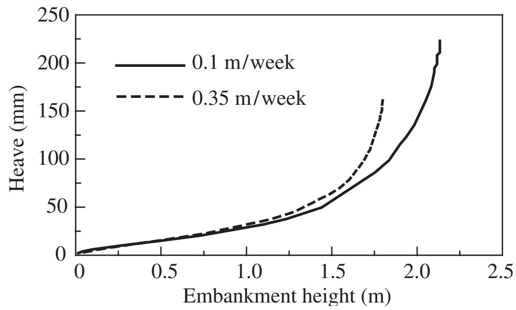

Figure 22. Heave at the toe of embankment.

because this gradual rate of construction allows the soft clay to gain shear strength upon pore pressure dissipation.

8.3. Influence of drain spacing

To investigate the effect of vertical drains on embankment stability, four different drain spacings were considered in the analysis; 1, 1.5, 2 and 3 m. The embankment is raised to a maximum height of 4 m, with two different construction rates, 0.1 m/week and 0.35 m/week. The slope of the embankment is assumed to be 2:1.

Figures 23 and 24 show the predicted surface settlement at the centerline and toe of the embankment, respectively. For a construction rate of 0.1 m/week, impending failure is not noticed for a small drain spacing of up to 2 m, which suggests that the higher dissipation of pore pressure and slower construction rate allow the soft clay foundation to gain sufficient strength to support a 4 m high embankment. If the construction rate is increased to 0.35 m/week, the foundation stabilized with PVD at 1 m spacing reaches its ultimate settlement within a shorter period (100 days) compared to a construction rate of 0.1 m/week

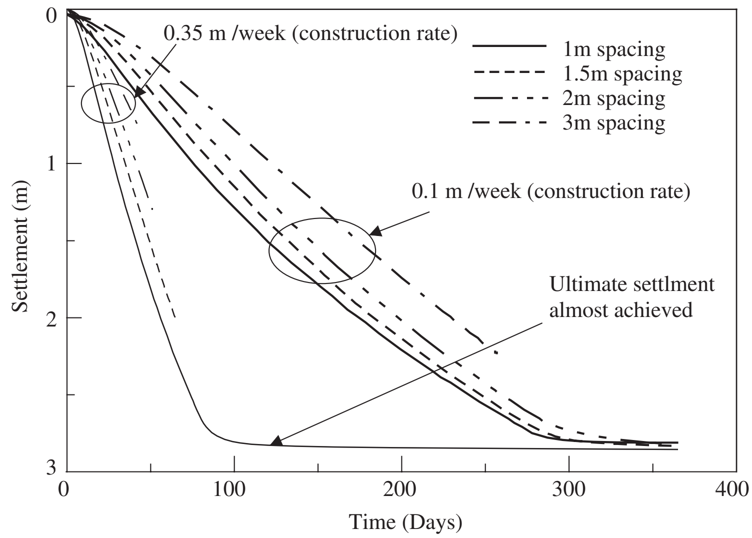

Figure 23. Predicted centerline surface settlement for different drain spacing.

(300 days). It is not possible to reach the final embankment height of 4 m if the drain spacing is 1.5, 2 or 3 m (Figure 24b).

9. PERFORMANCE OF TEST EMBANKMENTS CONSTRUCTED ON SOFT MARINE CLAY IN MALAYSIA

To study the performance and cost effectiveness of various ground improvement methods, in 1986 the Malaysian Highway Authority constructed a series of 15 trial embankments in Muar clay with nine different ground improvement techniques. The site of the test embankment is about 500 km east of Malacca on the southwest coast of Malaysia (Figure 25). The finite element program ABAQUS is used to predict the behavior of two of these embankments; one without any foundation improvement (i.e. north of embankment #1 in Figure 25), the other with geosynthetic vertical drains (PVD) at 1.3 m spacing installed in a triangular pattern (i.e. #14 in Figure 25).

9.1. Embankment constructed to failure

This embankment is shown in Figure 25, and is located just north of embankment #1. The cross-section of embankment showing the key instruments with subsoil variation, and the discretized finite element mesh, are shown in Figures 26 and 27, respectively. The piezometers P5, P6 and the inclinometers I3, I4 are used to monitor embankment failure. The

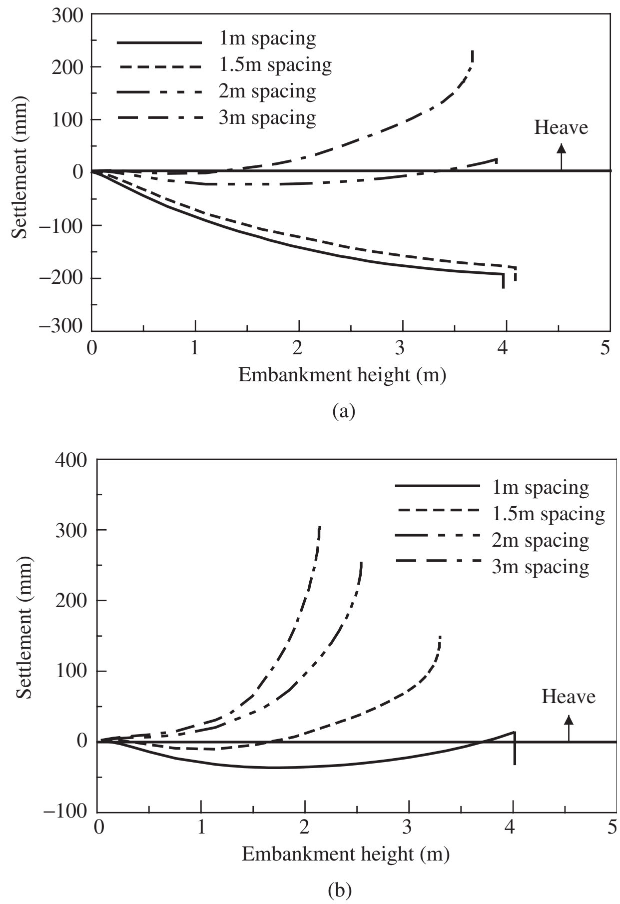

Figure 24. Predicted surface settlement at toe for different drain spacing at a construction rate of (a) 0.1 m/week, (b) 0.35 m/week.

embankment was raised with a fill material of 20.5 kN/m^3 bulk unit weight at a constant rate of 0.4 m/week (Indraratna et al., 1992). The MCC parameters and the in situ stresses are given in Tables 6 and 7, respectively.

The excess pore pressure variation along the embankment centerline, the surface settlement, and the lateral displacement at 10 m from the centerline are plotted in Figures 28–30 for a fill height of 5 m. As expected, the lateral displacement is significantly reduced in the stiffer clay layer. In general, the MCC theory overestimates the lateral displacements. The reason for this discrepancy can be attributed to several factors, including the lateral variability of soil parameters, the use of a simplified associated flow rule, and the effect of the stiff surficial crust (Potts and Zdravkovic, 2001). It was found that lateral

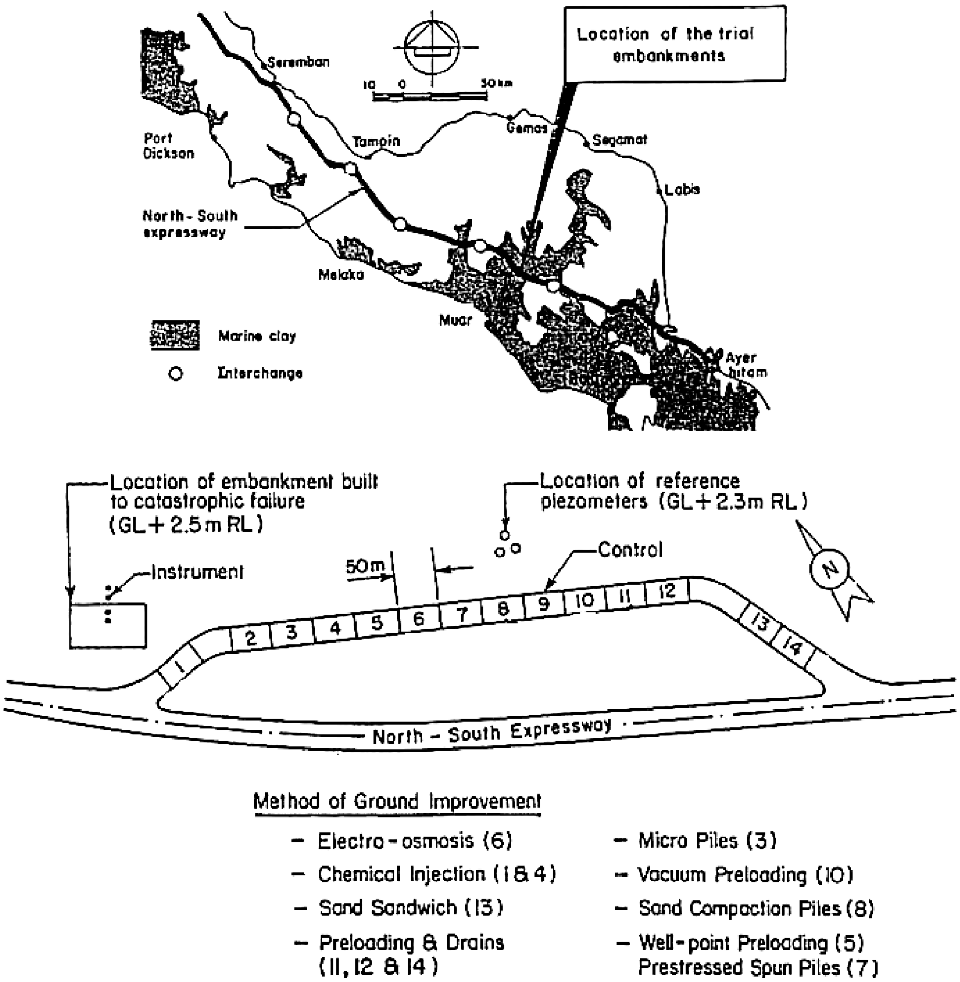

Figure 25. Location of Marine clay deposits and relative location of trial embankments along North–South expressway, Malaysia (modified after Indraratna et al., 1997).

displacements are also sensitive to nominal changes of compression parameter λ (Indraratna et al., 1992).

9.2. Embankment stabilized with geosynthetic vertical drain

The location of this embankment is shown in Figure 25 as embankment # 14. The embankment cross-section with key instrumentation and the associated subsoil profile is shown in Figure 31. The equivalent drain radius based on Eq. (4) is estimated to be r_w=0.03 m and the smear zone radius is taken as r_s=0.15 m. The Cam-clay parameters and equivalent

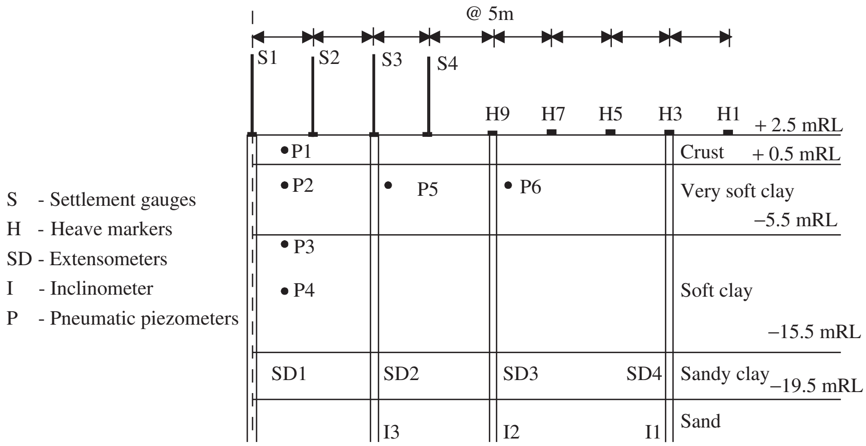

Figure 26. Cross-section of the failed embankment showing key instrumentations (modified after Indraratna et al., 1992).

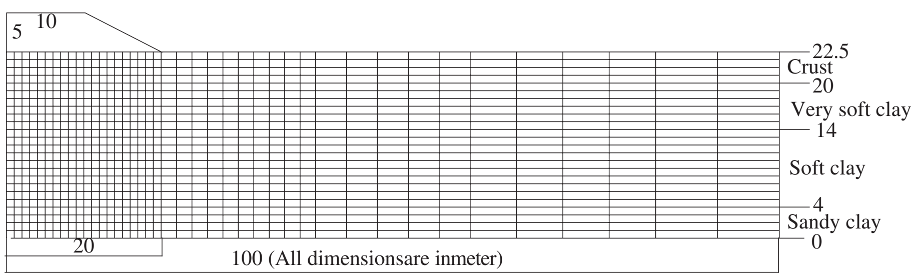

Figure 27. Finite element mesh for embankment constructed to failure.

Table 6. Soil parameters used in finite element analysis

Depth	k	λ	e_{cs}	M	ν	γ_s (kN/m^3)	k_h (m/s)	k_v (m/s)
0–2.5	0.05	0.13	3.07	1.19	0.3	16.5	1.5×10^{-9}	0.8×10^{-9}
2.5–8.5	0.05	0.13	3.07	1.19	0.3	15.5	1.5×10^{-9}	0.8×10^{-9}
8.5–18.5	0.08	0.11	1.61	1.07	0.3	15.5	1.1×10^{-9}	0.6×10^{-9}
18.5–22.5	0.10	0.10	1.55	1.04	0.3	16.0	1.1×10^{-9}	0.6×10^{-9}

Source: Indraratna and Sathananthan (2003)

plain strain permeabilities based on Eq. (30) are given in Table 8. Table 9 tabulates the in situ stress distribution. Embankment construction was carried out in two loading stages; during the first 14 days the height was raised to 2.57 m (Stage 1), and after a 90 day rest period the height was raised to 4.74 m in 24 days (Stage 2).

Table 7. In situ stress condition

Depth (m)	σ_{h0} (kPa)	σ_{v0} (kPa)	u (kPa)	P′c (kPa)
0	0	0	0	110
2.5	13.2	22.0	16.7	110
8.5	33.7	56.1	75.5	40
18.5	67.9	113.1	173.6	60
22.5	81.5	135.9	212.9	60

Source: Indraratna and Sathananthan (2003)

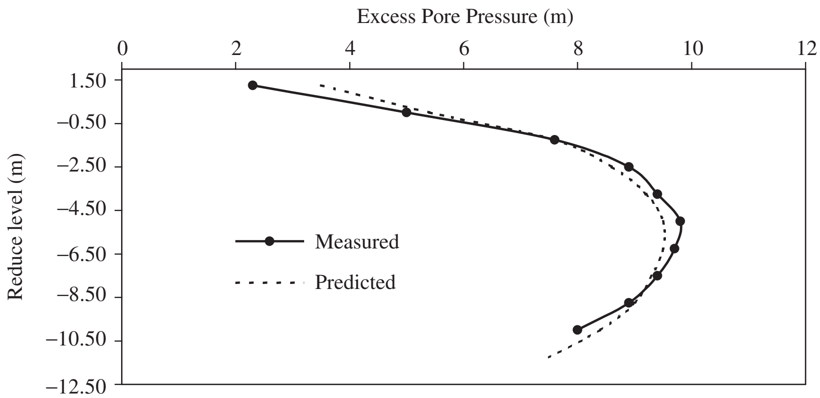

Figure 28. Excess pore pressure variation under embankment centerline.

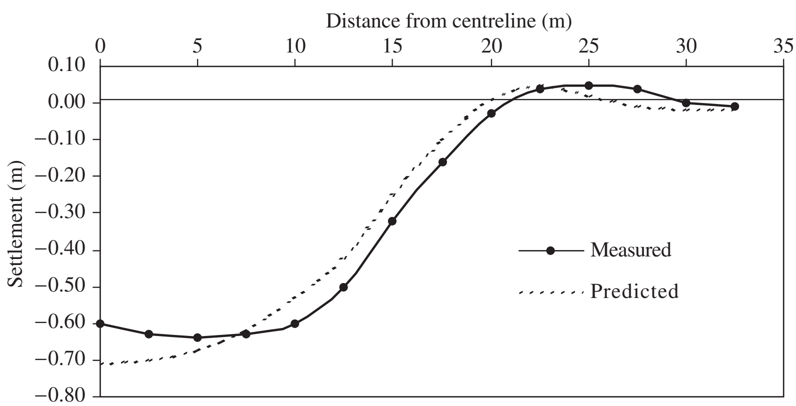

Figure 29. Surface settlement variation.

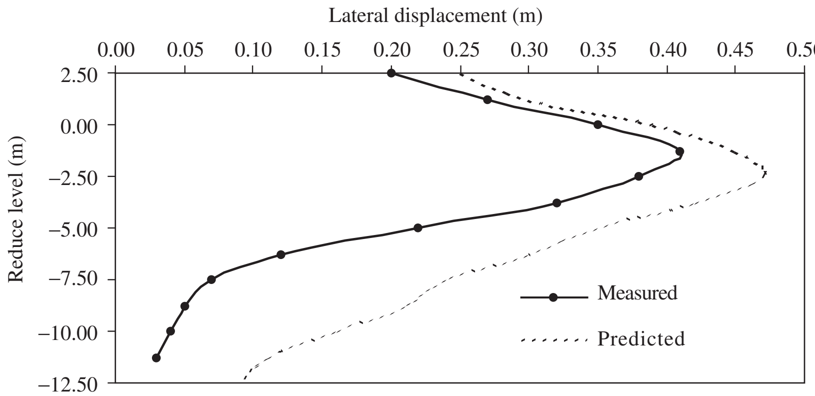

Figure 30. Lateral displacement profile at 10 m from centerline.

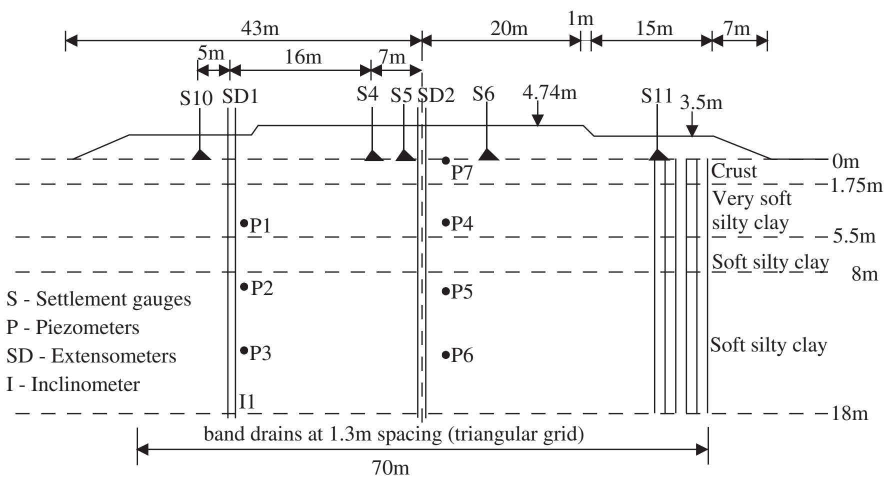

Figure 31. Cross-section of test embankment with key instrumentation (modified after Indraratna et al., 1994).

The finite element mesh of the embankment is shown in Figure 32 and the location of inclinometer (ID1-23 m away from the centerline) and piezometers are conveniently defined at mesh nodes. The well resistance of the drain was included because they were 18 m long. The well resistance was simulated by considering the vertical permeability of the transformed drain wall as previously discussed in Eq. (31c). The equivalent coefficient of permeability of drain was estimated as 0.0005 m/s by a single drain analysis.

The predicted and measured settlements at the centerline and along the surface are shown in Figures 33 and 34, respectively. Heave is also predicted beyond the toe of the

Table 8. Soil parameters used in finite element analysis

Depth (m)	κ	λ	e_{cs}	M	ν	γ_s	Permeability (10^{-9} m/s)			
							k_h	k'_h	k_{hp}	k'_{hp}
0–1.75	0.06	0.30	3.10	1.19	0.29	15.0	6.4	3.0	2.45	0.60
1.75–5.50	0.06	0.60	3.10	1.19	0.31	15.0	5.2	2.7	1.36	0.58
5.50–8.0	0.05	0.30	3.06	1.12	0.29	15.5	3.1	1.4	0.81	0.29
8.0–18.0	0.04	0.35	1.61	1.07	0.26	16.0	1.3	0.6	0.34	0.13

Source: Indraratna and Sathananthan (2003)

Table 9. In situ stress condition

Depth (m)	σ'_{v0} (kPa)	σ'_{h0} (kPa)	u (kPa)	P'_c (kPa)
0	0	0	0	110
1.75	28.6	17.3	0	95
5.50	48.4	29.1	36.7	44
8.0	62.6	37.6	61.3	60
18.0	124.6	74.8	159.3	135

Source: Indraratna et al. (1994)

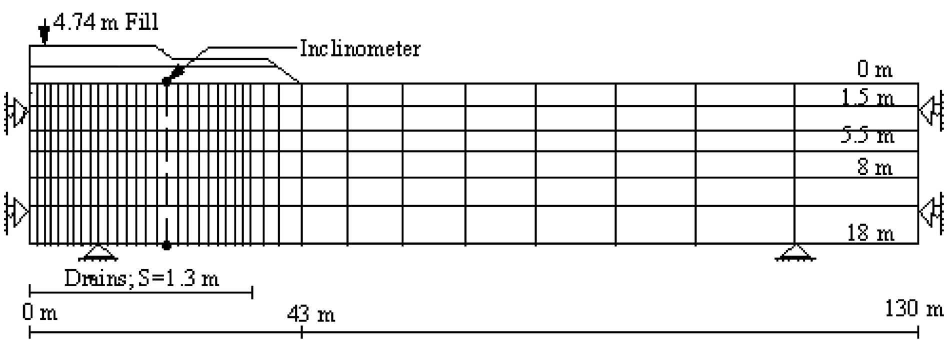

Figure 32. Finite element mesh used in plane strain analysis (adapted after Indraratna et al., 2000).

embankment, i.e. at about 45 m away from the centerline but regrettably, no field data were available for comparison. The predictions acceptably agree with the limited field measurements obtained near the centerline.

The evaluated and measured excess pore water pressure variations are shown in Figure 35. The measured excess pore pressure does not indicate much dissipation during Stage 2 due to the piezometer malfunctioning. Even though the prediction of excess pore pressure is made accurately in Stage 1 by including the smear effect, the predicted postconstruction pore pressure only improved slightly by including both smear and well resistance. As expected, the “perfect drain” underestimates the measurements. Observed and predicted lateral

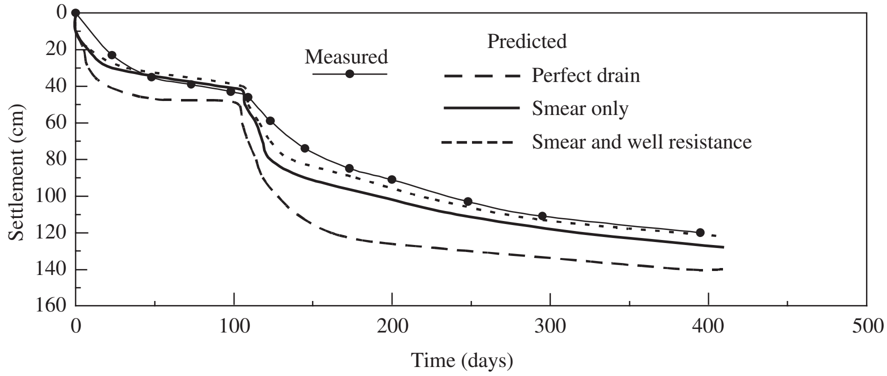

Figure 33. Settlement at embankment centerline.

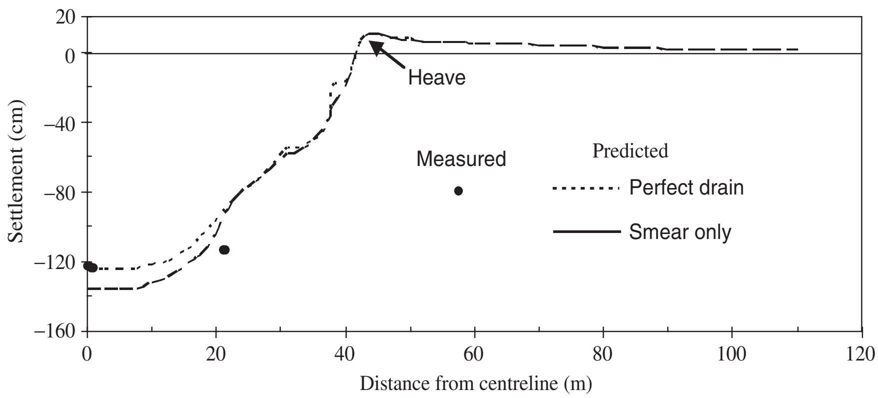

Figure 34. Surface settlement profile after 400 days.

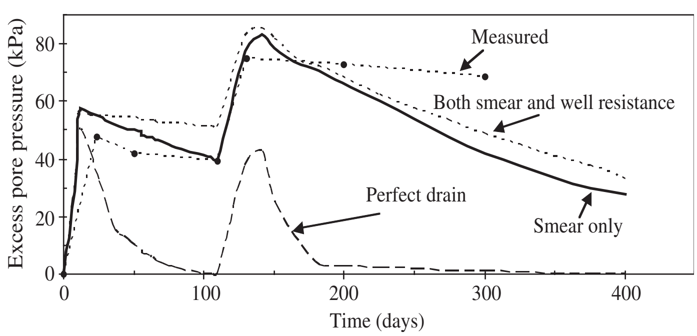

Figure 35. Excess pore water pressure variation at piezometer location, P6.

deformations are plotted in Figure 36. Acceptable agreement between the field data and predictions is obtained when both the smear and well resistance are considered. The perfect drain condition gives the smallest lateral deformation while maximizing vertical deformation.

9.3. Normalized deformation factors

The lateral displacement and settlement can be normalized with respect to the corresponding fill height to examine the effectiveness of the ground improvement techniques. Thus, the following "stability" indicators are defined (Indraratna et al., 1997): β_1, the ratio between lateral displacement and the corresponding fill height, β_2 the ratio between settlement and the corresponding fill height, and $\alpha = \beta_1/\beta_2$.

Figure 37 shows variation of β_1 with depth and Figure 38 shows the variation of α with depth. The normalized displacement of PVD-stabilized embankment is considerably less than an embankment constructed to failure. These results clearly show that vertical drains effectively decrease lateral deformations and enable the critical height of an embankment

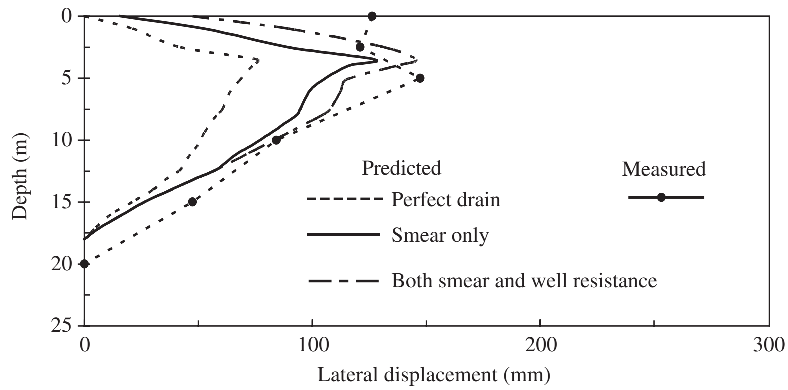

Figure 36. Lateral displacement profile after about 300 days at Inclinometer I1.

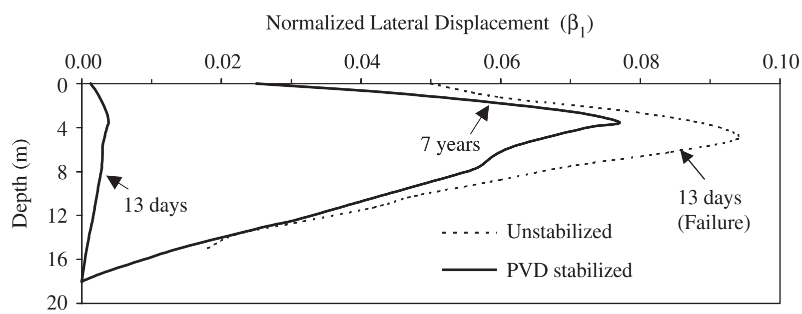

Figure 37. Normalized lateral displacement.

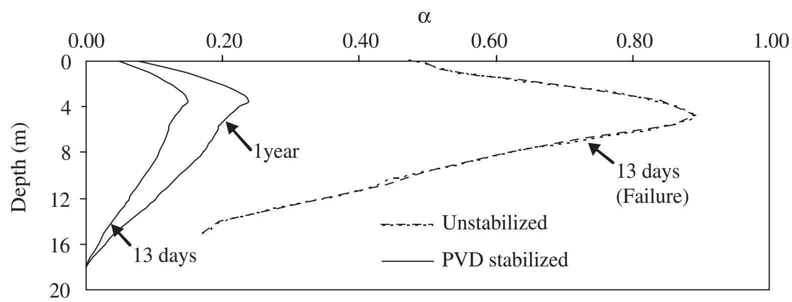

Figure 38. The variation of lateral displacement/settlement ratio with depth.

Table 10. Normalized deformation factors (modified after Indraratna et. al., 1997)

Ground improvement scheme	α	β_1	β_2
Sand compaction piles for pile/soil stiffness ratio of 5 (*h*=9.8 m, including 1 m sand layer)	0.185	0.018	0.097
Geogrids + vertical band drains in square pattern at 2.0 m spacing (*h*=8.7 m)	0.141	0.021	0.149
Vertical band drains in triangular pattern at 1.3 m spacing (*h*=4.75 m)	0.127	0.035	0.275
Embankment rapidly constructed to failure on untreated foundation (*h*=5.5 m)	0.695	0.089	0.128

to be increased. After 13 days, the untreated embankment fails with unacceptably large lateral displacement (Figure 37). The PVD-stabilized foundation takes more than 7 years before lateral displacement become similar to the failed embankment.

The normalized deformation factors for a few trial embankments are also compared in Table 10. In comparison with the unstabilized embankment constructed to failure, the stabilized foundations are characterized by considerably smaller values for α and β_1, which elucidates their obvious implications on stability. The normalized settlement (β_2) on its own is not a proper indicator of instability but is still a useful stability indicator when taken in conjunction with α and β_1. For example, the foundation having SCP gives the lowest values of β_1 and β_2, clearly suggesting the benefits of sand compaction piles over band drains.

10. CONCLUDING REMARKS

In this chapter, the use of prefabricated vertical drains, their properties and associated merits and demerits have been discussed. The behavior of soft clay under the influence of PVD was described on the basis of numerous case histories where both field measurements and numerical predictions were available. A sophisticated 3-D multidrain analysis with an individual axisymmetric zone of influence, with smear for each and every drain, will easily exceed computational capacity when applied to a real embankment project with a large number of PVD. In this context, the equivalent plane strain models will continue to offer a sufficiently accurate predictive tool for design, performance verification, and back analysis.

Selected numerical studies have been carried out to study the effect of embankment slope, construction rate, and drain spacing on the failure of soft clay foundations. Finally, the observed and the predicted performances of well-instrumented full-scale trial embankments built on soft Malaysian marine clay have been discussed using the plane strain theory. The numerical results based on ABAQUS conclude that the inclusion of both smear and well resistance improves the accuracy of the predicted settlement, excess pore pressures, and lateral deformation. As expected, the perfect drain analysis always overpredicts settlement and underpredicts excess pore pressures. The results presented here reaffirm that the effects of soil disturbance (smear) and well resistance are important for estimating deformation. While an accurate prediction of surface settlement is generally feasible, the acceptable prediction of lateral displacement is often difficult due to inherent assumptions made in the plane strain models. An accurate prediction of lateral displacement undoubtedly depends on the correct assessment of the value of λ of the MCC model, and the discharge capacity of PVD, among other parameters.

ACKNOWLEDGMENTS

The authors acknowledge the Malaysian Highway Authority for providing the trial embankments data. Significant extracts and adaptations of technical content of this chapter have come from the authors' previous publications such as the ASCE and Canadian Geotechnical Journal papers, as cited in the text and listed in the section.

REFERENCES

Aboshi, H. & Yoshikuni, H. (1967) A study in the consolidation process affected by well resistance in the vertical drain method*, Soils Found.s*, **l7**(4), 38–58.

Akagi, T. (1977) *Effect of Mandrel-Driven Sand Drains on Strength*, Proc. 9th International Conference on Soil Mech. and Found. Eng., Tokyo, **Vol. 1**, pp. 3–6.

Almeida, M.S.S. & Ferreira, C.A.M. (1993) *Field In Situ and Laboratory Consolidation Parameters of a Very Soft Clay*, Predictive Soil Mechanics, Proceedings of the Worth Memorial Symposium, Thomas Telford, London, pp 73–93.

Atkinson, M.S. & Eldred, P.J.L. (1981) Consolidation of soil using vertical drains, *Geotechnique*, **31**(1), 33–43.

Bamunawita, C. (2004) Soft clay foundation improvement via prefabricated vertical drains and vacuum preloading. PhD thesis, University of Wollongong, Australia. p.288.

Barron, R.A. (1948) Consolidation of fine-grained soils by drain wells, *Trans. ASCE*, 113 (paper 2346), 718–724.

Bergado, D. T., Asakami, H., Alfaro, M. C. & Balasubramaniam, A. S. (1991) Smear effects of vertical drains on soft Bangkok clay, *J. Geotech. Eng., ASCE*, **117**(10), 1509–1530.

Bergado, D.T. & Long, P.V. (1994) *Numerical Analysis of Embankment on Subsiding Ground Improved by Vertical Drains and Granular Piles*, Proceedings of 13th ICSMFE, New Delhi, India, pp 1361–1366.

Bergado, D.T., Manivannan, R. & Balasubramaniam, A. S. (1996) Proposed criteria for discharge capacity of prefabricated vertical drains, *J. Geotext. Geomembrances*, **14,** 481–505.

Carillo, N. (1942) Simple two and three dimensional cases in the theory of consolidation of soils, *J. Math. and Phys.*, **21**(1), 1–5.

Carroll, R.G. (1983) Geotextile filter criteria, *Transport. Res. Rec.,* **916**, TRB 46–53.

Chai, J.C. & Miura, N. (1999) Investigation of factors affecting vertical drain behavior, *J. Geotech. Eng.*, ASCE, **125**(3), 216—226.

Chai, J. C., Miura, N., Sakajo, S. & Bergado, D. (1995) Behavior of vertical drain improved subsoil under embankment loading. *J. Soil Found.*, Japanese Geotechnical Society, **35**(4), 49–61.

Chai, J.C., Shen, S.L., Miura, N. & Bergado, D.T. (2001) Simple method of modelling PVD improved subsoil, *J. Geotech. Eng., ASCE*, **127**(11), 965–972.

Christopher, B.R. & Holtz, R.D. (1985) *Geotextile Engineering Manual*, U.S. Federal Highway Administration, Report No. FHWA-TS-86/203, 1044 pp.

de Jager, W.F.J. & Oostveen, J.P. (1990) *Systematic Quality Control of Vertical Drains*, Proceedings 4th International conference on Geotextiles, Geomembranes and Related Products, The Hague, pp 321–326.

Dunnicliff, J. (1988) *Geotechnical Instrumentation for Monitoring Field Performance*, A Wiley Interscience, New York, p 577.

Hanna, T.H. (1985) *Field instrumentation in Geotechnical Engineering*, Trans Tech Publications, Germany, 843 pp.

Hansbo, S. (1979) Consolidation of clay by band-shaped prefabricated drains. *Ground Eng*., **12**(5), 16–25.

Hansbo, S. (1981) *Consolidation of Fine-Grained Soils by Prefabricated Drains*, Proceedings of 10th International Conference on SMFE., Stokholm, **Vol. 3**, pp 677–682.

Hansbo, S. (1987) *Design Aspects of Vertical Drains and Lime Column Installation*, Proceedings of 9th Southeast Asian Geotechnical Conference, **Vol. 2**, No. 8, pp 1–12.

Hansbo, S. (1997) Aspects of vertical drain design: Darcian or non-Darcian flow, *Geotechnique*, **47**(5), 983–992.

Hibbitt, K.& Sorensen (2004) *ABAQUS/Standard User's Manual*, HKS Inc.

Hird, C.C. & Moseley, V.J. (2000) Model study of seepage in smear zones around vertical drains in layered soil, *Geotechnique* **50**(1), 89–97.

Hird, C.C., Pyrah, I.C. & Russell, D. (1992) Finite element modelling of vertical drains beneath embankments on soft ground, *Geotechnique*, **42**(3), 499–511.

Holtz, R.D. & Holm, G. (1973) *Excavation and Sampling Around Some Sand Drains at Ska-Edeby*, Sweden, Proceedings of Specialty Conference on Performance on Earth and Earth supported Structure, Purdue University, **Vol. 1**, pp 435–464.

Holtz, R.D., Jamiolkowski, M., Lancellotta, R. & Pedroni, S. (1989) *Behaviour of Bent Pvd's*, Proceedings of 12th ICSMFE, Rio De Janeiro, **Vol. 3**, pp 1657–1660.

Holtz, R.D., Jamiolkowski, M., Lancellotta, R. & Pedroni, S. (1991) Prefabricated vertical drains: Design and performance, *CIRIA Ground Engineering Report: Ground Improvement,* Butterworth-Heinemann Ltd, UK, 131 pp.

Indraratna, B., Balasubramaniam, A. S. & Balachandran, S. (1992) Performance of test embankment constructed to failure on soft marine clay, *J. Geotech. Eng., ASCE*, **118**(1), 12–33.

Indraratna, B., Balasubramaniam, A. S. & Ratnayake, P. (1994) Performance of embankment stabilized with vertical drains on soft clay, *J. Geotech. Eng., ASCE*, **120**(2), 257–273.

Indraratna, B., Balasubramaniam, A. S. & Sivaneswaran, N. (1997) Analysis of settlement and lateral deformation of soft clay foundation beneath two full-scale embankments. *Int. J. Numer. Anal. Met. Geomech.* **21**, 599–618.

Indraratna, B. & Redana, I. W. (1995) Large-scale, radial drainage consolidometer with central drain facility, *Australian Geomech.,* **29**, 103–105.

Indraratna, B. & Redana, I. W. (1997) Plane strain modeling of smear effects associated with vertical drains, *J. Geotech. Eng., ASCE*, **123**(5), 474–478

Indraratna, B. & Redana, I. W. (1998) Laboratory determination of smear zone due to vertical drain installation, *J. Geotech. Eng., ASCE*, **125**(1), 96–99.

Indraratna, B. & Redana, I. W. (2000) Numerical modeling of vertical drains with smear and well resistance installed in soft clay, *Can. Geotech. J.*, **37**, 132–145.

Indraratna, B., Rujikiatkamjorn, C. & Sathananthan, I. (2005) *Analytical Modeling and Field Assessment of Embankment Stabilized with Vertical Drains and Vacuum Preloading,* Proceedings of the 16th International Conference on Soil Mechanics and Geotechnical Engineering, Osaka, Japan, submitted.

Indraratna, B., Rujikiatkamjorn, C., Sathananthan, I. & Shahin, M.A. (2005) *Analytical and Numerical Solutions for Soft Clay Consolidation Using Geosynthetic Vertical Drains with Special Reference to Embankments*, 5th International Geotechnical Conference, Cairo, pp 55–86.

Indraratna, B. & Sathananthan, I. (2003) *Comparison of field measurements and predicted performance beneath full scale embankments*, Proceedings of the 6th international symposium on field measurements in geomechnics, Oslo, Norway. pp 117–126.

Indraratna, B. & Sathananthan, I. (2004) *Numerical Prediction of Soft Clay Consolidation with Geosynthetic Vertical Drains Using Plane Strain Solution*, Proceeding, 9th ANZ Conference on Geomechanics, Auckland, Newzealand, pp 633–639.

Jamiolkowski, M. & Lancellotta, R. (1981) *Consolidation by Vertical Drains - Uncertainties Involved in Prediction of Settlement Rates*, Panel Discussion, Proceedings of the 10th International Conference on Soil Mech. and Found. Eng., Stockholm, **Vol. 1**, pp 345–451.

Jamiolkowski, M., Lancellotta, R. & Wolski, W. (1983) *Precompression and Speeding up Consolidation*, Proceedings of the 8th Eropean Conf. Soil Mech. And Found. Eng., Helsinki, **Vol. 3**, Spec. Session No. 6, pp 1201–1226.

Kim, Y.T. & Lee, S.R. (1997) An equivalent model and back-analysis technique for modelling in situ consolidation behavior of drainage-installed soft deposits, *Comput. Geotech.*, **20**(2), 125–142.

Kjellman, (1948) *Accelerating Consolidation of Fine Grain Soils by Means of Cardboard Wicks*, Proceedings of the 2nd ICSMFE, **Vol. 2**, pp 302–305.

Kremer, R., de Jager, W., Maagdenberg, A., Meyvogel, I. & Oostveen, J. (1982) *Quality Standards for Vertical Drains*, Proceedings, 2nd International Conference on Geotextile, Las Vegas, pp 319–324.

Kremer, R., Oostveen, J., Van Weele, A.F., de Jager, W. & Meyvogel, I. (1983) *The Quality of Vertical Drainage*,. Proceedings, 8th European Conference on SMFE, Helsinki, **Vol. 2**, pp 721–726.

Lau, K.W.K. & Cowland, J.W. (2000) Geosynthetically enhanced embankments for the Shenzhen river, *Adv. Transport. and Geoenviron. Systems Geosynth.*, Geotechnical Special Publication no. **103,** 140—161 pp.

Lin, D.G., Kim, H.K. & Balasubramaniam, A.S. (2000) Numerical modelling of prefabricated vertical drain. *Geotech. Eng. J., Southeast Asian Geotechnical Society*, **31**(2), 109–125.

Long, R.P. & Covo, A. (1994) *Equivalent diameter of vertical drains with an oblong* cross section, *J. Geotech. Eng. Div., ASCE*, **120**(9), 1625–1630.

Mesri, G. & Lo, D.O.K. (1991) *Field Performance of Prefabricated Vertical Drains*, Proceeding International Conference on Geotechnical Engineering for Coastal Development-Theory to Practice, Yokohama, Japan, **Vol. 1**, pp 231–236.

Onoue, A. (1988) Consolidation by vertical drains taking well resistance and smear into consideration, *J. Soils Found.*, **28**(4), 165–174.

Onoue, A., Ting, N.H., Germaine, J.T. & Whitman, R.V. (1991) *Permeability of Disturbed Zone around Vertical Drains*, Proceeding of the ASCE Geot. Eng. Congress, Colorado, pp 879–890.

Potts, D. M. & Zdravković, L. (2001) *Finite Element Analysis in Geotechnical Engineering – application*, Thomas Telford Publishing, London.

Pradhan, T.B.S., Imai, G., Murata, T., Kamon, M. & Suwa, S. (1993) *Experiment Study on the Equivalent Diameter of a Prefabricated Band-Shaped Drain*, Proceedings of the 11th Southeast Asian Geotech. Conference, **Vol. 1**, pp 391–396.

Ratnayake, A.M.P. (1991) Performance of test embankments with and without vertical drains at Muar Flats site, Malaysia. MS thesis, AIT, Bangkok, Thailand.

Rendulic, L. (1936) *Relation between Void Ratio and Effective Principal Stresses for a Remoulded Silty Clay*, 1st International Conference on Soil Mechanics, Harvard, **Vol. 3**, pp 48–53.

Rixner, J.J., Kraemer, S.R. & Smith, A.D. (1986) *Prefabricated vertical drains, Vol. I, II and III*: Summary of Research Report-Final Report, Federal Highway Admin., Report No. FHWA-RD-86/169, Washington, DC, 433 pp.

Shinsha, H., Hara, H., Abe, T. & Tanaka, A. (1982) Consolidation Settlement and lateral displacement of soft ground improved by sand drains, *Tsuchi-to-Kiso*, *Japanese Soc. Soil Mech. Found. Eng.*, **30**(2), 7–12.

Stamatopoulos, A.C. & Kotzias, P.C. (1985) *Soil Improvement by Preloading*. Wiley, New York, p 261.

Terzaghi, K. & Peck, R.B. (1967) *Soil Mechanics in Engineering Practice*, 2 Edition, Wiley, New York, 729 pp.

Xiao, D. (2000) Consolidation of soft clay using vertical drains, PhD thesis, Nanyang Technological University, Singapore. p. 301.

Yoshikuni, H. & Nakanodo, H. (1974) Consolidation of fine-grained soils by drain wells with finite permeability, *Soil Mech. Found. Eng.*, **14**(2), 35–46.

Zeng, G.X. & Xie, K.H. (1989) *New Development of the Vertical Drain Theories.* Proceedings of the 12th International Conference on Soil Mechanics and Foundation Engineering, Rotterdam **Vol. 2**, pp 1435–1438.